Observation of Ion-Acoustic Shocks in a Dusty Plasma

Y. Nakamura and H. Bailung*
Institute of Space and Astronautical Science, Yoshinodai, Sagamihara, Kanagawa 229-8510, Japan

P. K. Shukla
Institut fuer Theoretische Physik IV, Ruhr Universitaet, Bochum, 44780 Bochum, Germany
(Received 20 January 1999)

Linear and nonlinear dust ion-acoustic waves are studied experimentally in a homogeneous unmagnetized dusty plasma. In the linear regime, the phase velocity of the wave increases and the wave suffers heavy damping with increasing dust density. An oscillatory ion-acoustic shock wave in usual Ar plasma transforms into a monotonic shock front when it travels through the dusty plasma column. The Korteweg–de Vries–Burgers equation is numerically integrated taking experimental parameters into account, and the results are compared with the experimental findings.

PACS numbers: 52.35.Fp, 52.35.Tc

Ion-acoustic solitons were first observed in a novel device called a double plasma device [1]. The characteristics such as the velocity and width of those solitons agreed well with the Korteweg–de Vries (KdV) equation [2]. Using the same double plasma device, Taylor *et al.* [3] excited an ion-acoustic shock wave by applying a ramp voltage to the anode of the driver plasma. The shock wave is possible when some ions are reflected by the shock front [4]. It is noted that the observed oscillatory shock structure is formed when the KdV equation is numerically integrated for an initial ramp voltage [5].

Recently, ion-acoustic shocks have been observed in Q-machine plasmas with negative ions [6,7]. Takeuchi *et al.* [6] measured a critical negative ion concentration ε_c above which a negative density jump showed a shocklike structure. They compared the measured ε_c with a KdV equation which does not possess a shock solution. Luo *et al.* [7] observed the formation of a shock structure by reduction rf Landau damping due to an increase of the electron to ion temperature ratio.

The dispersion of the ion-acoustic wave is normal, which balances the positive nonlinearity to form solitons. It is the physics behind the KdV equation. For a wave which possesses a positive nonlinearity like the ion-acoustic wave, damping like Landau damping or collisional damping is needed to form shock waves which results in the Burgers equation [8]. The Burgers equation has no dispersive term. However, since the ion-acoustic wave is dispersive, the dispersion must be taken into account. As a result of this, the KdV-Burgers equation [8] must be considered for the waves which have normal dispersion, positive nonlinearity, and a wave number dependent damping.

The purpose of the present work is to observe shock waves in an unmagnetized dusty plasma. The development of the shock is compared with the numerical integration of the KdV-Burgers equation.

The KdV-Burgers equation for our purpose is

$$\frac{1}{P}\frac{\partial \phi}{\partial \tau} + \phi\frac{\partial \phi}{\partial \xi} + \beta\frac{\partial^3 \phi}{\partial \xi^3} - \mu\frac{\partial^2 \phi}{\partial \xi^2} = 0, \quad (1)$$

where ϕ is the wave potential normalized with $\kappa T_e/e$ and the time and space variables are in the units of $1/\omega_{pi}$ and λ_e, respectively. Here T_e is the electron temperature, $\omega_{pi} = (4\pi n_i e^2/M)^{1/2}$ and $\lambda_e = (\kappa T_e/4\pi n_e e^2)^{1/2}$ are the ion plasma frequency and the electron Debye length, respectively, with $n_i = n_e + QN_d$ and Q is the number of charges residing on the dust grain, n_e, n_i, and N_d are the unperturbed number density of electrons, ions, and dust grains, respectively, and M is the ion mass. Experimentally the ion temperature T_i is much smaller than T_e. Then we can neglect T_i so that $P = 1$ and $\beta = \frac{1}{2}$. The coordinate ξ is moving with $(n_i/n_e)^{1/2}$. The dissipation coefficient μ is proportional to the collision frequency of ions. In deriving Eq. (1), we have assumed the Boltzmann distribution for the electrons [9], which is valid in the present case, i.e., the wavelength is shorter than $v_{\rm te}^2/C_s\nu_{\rm ed}$, where $v_{\rm te}$ is the electron thermal velocity and $\nu_{\rm ed}$ is the electron-dust collision frequency.

Equation (1) governs the dynamics of the nonlinear dust ion-acoustic waves in dusty plasmas in which collisions between stationary dust grains and ions are considered. When the dispersion term is not neglected compared with the dissipation term, Eq. (1) exhibits an oscillatory shock. On the other hand, when the dispersion is much weaker than the dissipation provided by the ion collisions, we can neglect the β term in Eq. (1) and the resulting equation becomes the Burgers equation, which admits a monotonic (laminar) shock that is well known in gas dynamics.

An example of the numerical solution of Eq. (1) for an initial ramp signal is shown in Fig. 1. In the absence of dust, i.e., when there is no dissipation, Eq. (1) transforms into a simple KdV form, and numerical results show an ion-acoustic shocklike wave at normalized time $\tau = 150$ with an oscillatory structure behind it. The oscillatory structure separates into individual solitons

 0031-9007/99/83(8)/1602(4)$15.00

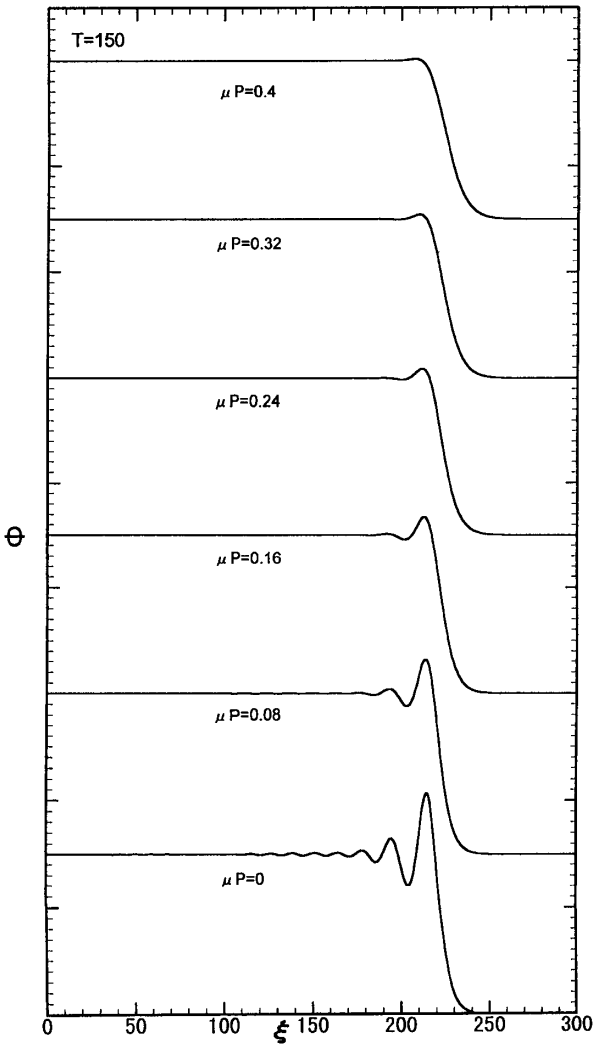

FIG. 1. Numerical results of KdV-Burgers equation [Eq. (1)] for an initial ramp signal with $\mu P = 0 \sim 0.4$ at time $T = 150$. The height of the ramp signal is 0.15.

when time passes and when nonlinearity is balanced by dispersion [5]. Numerical results for the values of $\mu P = 0.08$ and 0.32 at time $\tau = 150$ show a gradual decrease of the number of oscillations behind the shock front. Finally, when $\mu P > 0.40$ a monotonic shock front is produced. The increase of μ (the coefficient of the Burgers dissipation term) physically corresponds to the increase of dust density which in turn increases the ion-dust collision frequency. Our numerical results also coincide with the remark that for the KdV-Burgers equation there exists a critical value of μ at which an oscillatory shock transforms into a monotonic shock structure [8].

The experiment is carried out in a dusty double plasma device [10]. The inner diameter of the device is 40 cm and its length is 90 cm. The device is separated into a source and a target section by a fine mesh grid which is kept electrically floating. The chamber is evacuated down to 5×10^{-7} torr with a turbomolecular pump. Ar gas is bled into the chamber at a partial pressure $(4 \sim 5) \times 10^{-4}$ torr. A dust dispersing setup fitted at the target section is consisted of a dust reservoir coupled to an ultrasonic vibrator. The dust reservoir consists of a fine stainless steel mesh (300 lines per in.) of 10 cm (width) $\times$ 16 cm (axial length) area at the bottom end and is placed horizontally closer to the anode wall. It is kept electrically floating. The ultrasonic vibrator is tuned at 27 kHz to vibrate the dust reservoir by using a signal generator and a power amplifier. We use the glass powder of average diameter 8.8 μm of which full width at half maximum is 8 μm, and which falls uniformly through the mesh. The dust density is easily controlled by adjusting the power of the signal applied to the vibrator and is measured from the extincted intensity of a laser light which passes through the dust column and is collected by a photodiode array. The maximum dust density of the order of 10^5 cm^{-3} is obtained in this setup. Plasma parameters measured by a plane Langmuir probe of 6 mm diameter and a retarding potential analyzer are as follows: plasma density $n_e = 10^8 \sim 10^9$ cm^{-3}, electron temperature $T_e = 1 \sim 1.5$ eV, an ion temperature $T_i < 0.10$ eV. The number of charge $Q \approx 10^5$ for $N_d < 10^3$ cm^{-3}, and it reduces to a much smaller value 10^2 for $N_d \approx 10^5$ cm^{-3} [10,11].

We first measure the linear dispersion relation for dust ion-acoustic wave using an interferometer method for continuous small amplitude ($\approx$300 mV) sinusoidal waves of frequency 100 to 700 kHz. An example of the measured dispersion relations (Ω-K) is shown in Fig. 2.

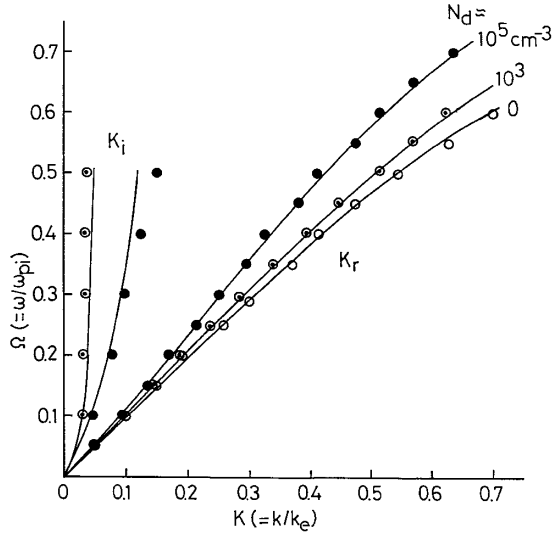

FIG. 2. Measured dispersion relations (filled circles) for dust ion-acoustic wave when $N_d \approx 10^3$ cm^{-3} ($n_i/n_e = 1.5$) and 10^5 cm^{-3} ($n_i/n_e = 1.8$). The open circles represent the no dust condition. The solid lines are theoretical with $\nu_i = 0$ (no dust condition, i.e., $n_i/n_e = 1$, lowest curve), 0.1 ($n_i/n_e = 1.5$) and 0.2 ($n_i/n_e = 1.8$), and $T_i/T_e = 0.1$. The measured K_i for same dust densities are also shown. Theoretical K_i correspond to $\nu_i = 0.1$ for $n_i/n_e = 1.5$ and 0.2 for $n_i/n_e = 1.8$.

The lower trace is for no dust condition with $T_i/T_e = 0.07$ and $\nu_i = 0$, where ν_i is the collision frequency of ions with the neutral atoms and dust particles normalized to ω_{pi}. In order to compare the experimental dispersion relation with theory, we consider a general dispersion relation for ion-acoustic waves in a dusty plasma as

$$1 = \frac{\omega_{pe}^2}{\omega^2 - k^2 v_e^2} + \frac{\omega_{pi}^2}{\omega^2 - 3k^2 v_i^2} + \frac{\omega_{pd}^2}{\omega^2 - 3k^2 v_d^2}, \tag{2}$$

where ω_{pj} ($j = e$, i, and d) represent the plasma frequency for the respective components, and $v_j = (\kappa T_j/m_j)^{1/2}$ with T_j and m_j are temperature and mass of the respective components.

We assume $\omega/k \ll v_e$ and neglect the third term of Eq. (2) because ω_{pd} is negligible compared with ω_{pi}, and thus obtain the dispersion relation for ion-acoustic wave modified by the presence of charged dust. The theoretical dispersion relations shown in Fig. 2 are obtained including the effect of collision of ions by substituting $\omega^2 = \omega(\omega + i\nu_i\omega_{pi})$ in the second term of Eq. (2). Comparison of the theoretical dispersion relations with corresponding experimental (n_i/n_e) suggests that ion-dust collision frequency increases with increasing dust density. It is also clearly seen that the phase velocity of the wave increases when dust density is increased. The increase in the phase velocity is attributed to the removal of free electrons by the dust grains which decreases the shielding effect. The measured normalized spatial damping K_i shown in Fig. 2 nearly coincides with theoretically calculated K_i for the same n_i/n_e with $\nu_i = 0.1$ and 0.2, respectively. The dusty plasma produced in the double plasma device thus possesses a noble medium where both the dispersion and the dissipation (collisional) effects are present to observe the numerical results of ion-acoustic shock transition described by the KdV-Burgers equation. The collision frequency of the ions is obtained empirically comparing the measured damping with Eq. (2).

An ion-acoustic shock wave is excited in the plasma by applying a ramp voltage with rise time ≈ 10 μsec to the driver anode. The Langmuir probe is biased above the plasma potential in order to detect the signal as fluctuations in the electron saturation current. The probe surface was repeatedly cleaned with an ion bombardment by applying -150 V. An example of the observed shock front is shown in Fig. 3(a) at different probe positions when dust is off. The applied ramp voltage has an amplitude of 2.0 V. As the wave propagates, the leading part steepens owing to nonlinearity ($X = 3$ cm), which makes the effect of dispersion larger. Then an oscillatory structure is formed due to the dispersion ($X = 5 \sim 11$ cm). The signal ($X = 13$ cm) is similar to that when $\mu P = 0$ in Fig. 1. Since the normalized perturbation $\delta n/n$ of electron density is much smaller than unity, $\delta n/n \approx \phi$. The big trough seen when $X = 5$ cm is an ion hole propagating with a speed slower than the ion-acoustic velocity. This observation is somewhat similar to the first observation of ion-acoustic shock by Taylor *et al.* [3]. An ion burst is also seen in front of the shock as a precursor which is recognized as a bunch of energetic ions generated due to the signal applied to the source anode relative to the target. This precursor plays a crucial role in enhancement of shock damping.

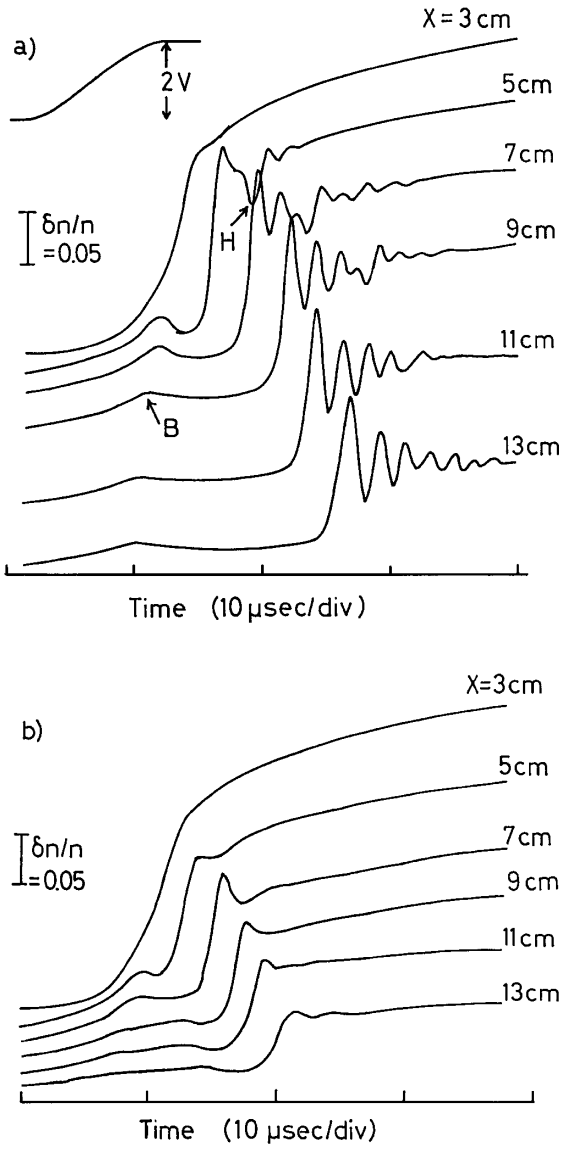

FIG. 3. Observed signals at different axial probe positions X which is measured from the grid. The delay time for successive signals (5 cm $\sim$ 13 cm) is shifted by 10 μsec to the left. Top trace is the applied signal. (a) Ion-acoustic oscillatory shock when $N_d = 0$. H is an ion hole and B is an ion burst. (b) Dust ion-acoustic shock when $N_d = 5 \times 10^4$ cm^{-3}. $\lambda_e = 0.06$ cm. $\omega_{pi} = 3.0 \times 10^5$ rad/s.

Under the same experimental condition, the modification of the propagation characteristics of the ion-acoustic shock wave is observed for a fixed dust density [Fig. 3(b)]. Near the grid (within 5 cm) the signal resembles the no-dust condition. However, when the shock travels more

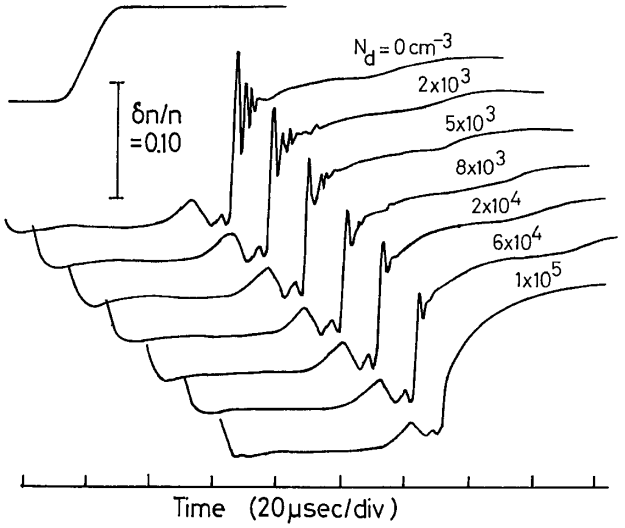

FIG. 4. Electron density versus time at a fixed probe position ($X = 12$ cm) showing the transition of an oscillatory shock to a monotonic shock when dust density is increased. Top trace is the applied ramp signal with amplitude =2.0 V and rise time ≈ 10 μsec.

than 7 cm through the dust column the steepening as well as the modification are clearly seen. At larger distances from the separation grid ($X = 9$ cm), the oscillatory wave structure behind the shock disappears since it has larger k so that its damping is larger than the shock structure due to the Burgers term and a monotonic shock front propagates. The same effect is also seen in the numerical results when the laminar shock is formed for higher values of μP (Fig. 1). The height of the flat part behind the shock front decreases when the wave propagates farther away from the grid. The spatial decrement of the height has been found to be nearly the same for both with and without dust. It is not due to the damping of the wave, but mainly due to a geometrical divergence since the grid dimension (40 cm in diameter) is finite. It has been confirmed with linear wave propagation in another device with grid diameter 60 cm.

To compare the observed effect of dust on the shock formation with the numerical results, we first excite the ion-acoustic shock in the plasma without dust and then increase the dust density at smaller steps keeping the probe fixed at $X = 12$ cm. The corresponding normalized time T $(= \omega_{pi}\tau)$ for the signal at $X = 12$ cm is about 150. Some of the signals corresponding to the best fit to the numerical parameters are shown in Fig. 4. It is clearly seen that the oscillatory wave structure behind the shock becomes less in number with increasing dust density, and finally completely disappears at a sufficiently high dust density leaving only the laminar shock front. The shock speed also increases with increasing dust density. It is also noted that the particle density behind the shock remains constant, although the amplitude of the shock front (steepened part) seems to decrease when dust density is increased.

The ion-acoustic wave is described with the KdV equation which gives soliton solutions. An oscillatory shock wave also results in such a plasma when a collisionless dissipation process exists either due to the reflection of ions from the potential barrier in the leading edge of the front or due to Landau damping. When the plasma composed of sufficiently high density charged dust, the ion-dust collision becomes larger and makes the Burgers dissipation term more effective than the KdV dispersion term to balance the nonlinearity, which results in the laminar shock. When the dust density is smaller, an intermediate state is observed.

The numerical result shows that a pure ion-acoustic shock wave transforms into a laminar shock when μ in the KdV-Burgers Eq. (1) increases. Measured linear dispersion relations confirm that μ is proportional to the ν_i of ions. In the experiment, the ion-dust collision is suitably controlled by controlling the dust density, and thereby the required dissipation to form the laminar shock is provided. The observed experimental results of the shock transition from oscillatory shock to a monotonic (laminar) shock via a KdV-Burgers shock formation are therefore qualitatively explained by the numerical results of the KdV-Burgers equation.

One of the authors, H. B. is thankful for support from DST, Government of India.

*Permanent address: IASST, Khanapara, Guwahati-22, Assam, India.

[1] H. Ikezi, R. J. Taylor, and D. R. Baker, Phys. Rev. Lett. **25**, 11 (1970).
[2] H. Washimi and T. Taniuti, Phys. Rev. Lett. **17**, 996 (1966).
[3] R. J. Taylor, D. R. Baker, and H. Ikezi, Phys. Rev. Lett. **24**, 206 (1970).
[4] S. S. Moiseev and R. Z. Sagdeev, J. Nucl. Energy, Part C **5**, 43 (1963).
[5] Y. Nakamura, *Nonlinear and Environmental Electromagnetics*, edited by H. Kikuchi (Elsevier Science Publishers, Amsterdam, 1985), p. 139.
[6] T. Takeuchi, S. Izuka, and N. Sato, Phys. Rev. Lett. **80**, 77 (1998).
[7] Q-Z. Luo, N. D'Angelo, and R. L. Merlino, Phys. Plasmas **5**, 2868 (1998).
[8] V. I. Karpman, *Nonlinear Waves in Dispersive Media* (Pergamon, Oxford, 1975), p. 101.
[9] P. K. Shukla and S. G. Tagare, Phys. Lett. **59A**, 38 (1976).
[10] Y. Nakamura and H. Bailung, Rev. Sci. Instrum. **70**, 2345 (1999).
[11] B. Walch, M. Horanyi, and S. Robertson, IEEE Trans. Plasma Sci. **22**, 97 (1994).